ACS APPLIED MATERIALS & INTERFACES

Research Article

www.acsami.org

Bioinspired Quercitrin Nanocoatings: A Fluorescence-Based Method for Their Surface Quantification, and Their Effect on Stem Cell Adhesion and Differentiation to the Osteoblastic Lineage

Alba Córdoba,[†,‡] Marta Monjo,[*,†,‡] Margarita Hierro-Oliva,[§,∥] María Luisa González-Martín,[§,∥] and Joana Maria Ramis[*,†,‡]

[†]Group of Cell Therapy and Tissue Engineering, Research Institute on Health Sciences (IUNICS), University of Balearic Islands, Carretera de Valldemossa km 7.5, 07122 Palma de Mallorca, Spain

[‡]Instituto de Investigación Sanitaria de Palma, 07010 Palma de Mallorca, Spain

[§]Departamento de Física Aplicada, Facultad de Ciencias, Universidad de Extremadura, 06071 Badajoz, Spain

[∥]Biomedical Research Networking Center in Bioengineering, Biomaterials and Nanomedicine (CIBER-BBN), 50018 Zaragoza, Spain

Supporting Information

ABSTRACT: Polyphenol-based coatings have several potential applications in medical devices, such as cardiovascular stents, contrast agents, drug delivery systems, or bone implants, due to the multiple bioactive functionalities of these compounds. In a previous study, we fabricated titanium surfaces functionalized with flavonoids through covalent chemistry, and observed their osteogenic, anti-inflammatory, and antifibrotic properties in vitro. In this work, we report a fluorescence-based method for the quantification of the amount of flavonoid grafted onto the surfaces, using 2-aminoethyl diphenylborinate, a boronic ester that spontaneously forms a fluorescent complex with flavonoids. The method is sensitive, simple, rapid, and easy to perform with routine equipment, and could be applied to determine the surface coverage of other plant-derived polyphenol-based coatings. Besides, we evaluated an approach based on reductive amination to covalently graft the flavonoid quercitrin to Ti substrates, and optimized the grafting conditions. Depending on the reaction conditions, the amount of quercitrin grafted was between 64 ± 10 and 842 ± 361 nmol on 6.2 mm Ti coins. Finally, we evaluated the in vitro behavior of bone-marrow-derived human mesenchymal stem cells cultured on the quercitrin nanocoated Ti surfaces. The surfaces functionalized with quercitrin showed a faster stem cell adhesion than control surfaces, probably due to the presence of the catechol groups of quercitrin on the surfaces. A rapid cell adhesion is crucial for the successful performance of an implant. Furthermore, quercitrin-nanocoated surfaces enhanced the mineralization of the cells after 21 days of cell culture. These results indicate that quercitrin nanocoatings could promote the rapid osteointegration of bone implants.

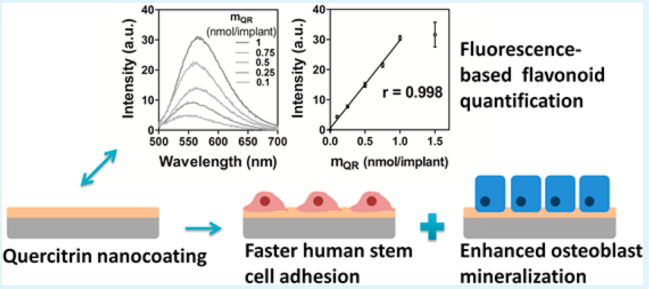

KEYWORDS: *flavonoids, polyphenols, biomaterial, DPBA, implant*

INTRODUCTION

In the past two years the potential of polyphenol-based coatings in medical devices has been raised, with applications in selectively bioactive cardiovascular stents,[1] stable and water-dispersible contrast agents,[2] antifouling surfaces,[3] or cancer-targeted nanoparticles.[4]

Flavonoids are a large family of natural small polyphenolic molecules, with a broad range of bioactivities. They are secondary plant metabolites that are present in the daily human diet, e.g., in fruits, vegetables, seeds, wine, or tea, and have known antioxidant, anti-inflammatory, and antibacterial properties.[5] High flavonoid intakes have been related to the prevention of cancers and cardiovascular diseases, to neuroprotective and antiaging effects, and to beneficial effects on the metabolism of bone. As potential drugs, they have also shown antiviral, antiulcer, antiosteoporotic, antiallergic, and antihepatotoxic properties.[6]

It has recently been reported that several plant-derived polyphenols are able to form coatings by self- assembly on different substrates, although it is not clear yet which is the assembling mechanism and the coating structure.[7−9] Besides, the obtainment of reversible thin metal−polyphenol films formed by coordination, which could be used in drug delivery systems, has also been reported.[10]

In a recent work, we functionalized Ti surfaces with flavonoids quercitrin and taxifolin. The surfaces showed

Received: June 9, 2015
Accepted: July 13, 2015
Published: July 13, 2015

DOI: 10.1021/acsami.5b05044
ACS Appl. Mater. Interfaces 2015, 7, 16857−16864

promising bone-stimulating, anti-inflammatory, and antifibrotic effects in vitro, on human mesenchymal stem cells (hMSCs) derived from umbilical cord, and human gingival fibroblasts cultured on the surfaces.[11] Furthermore, the biological effects were similar to those observed previously on cells treated with these flavonoid compounds in solution,[12−14] proving that the covalent immobilization of flavonoids to a surface through its ketone group does not impair its bioactive behavior. These multifunctional bioactive flavonoid-modified surfaces could have a potential application in bone implant surfaces to decrease the risk of implant failure, since the main causes of bone implant failure are related either to a fibrous tissue integration around the implant, which causes an encapsulation of the implant, or to the occurrence of inflammatory procedures or bacterial infections such as peri-implantitis.

Quantitative techniques for the determination of surface coverage in functionalized substrates are usually expensive and time-consuming and need large and specialized equipment and technicians that are not always easily available. Fluorescence spectroscopy is a very sensitive routine technique, commonly available in all research laboratories. 2-Aminoethyl diphenylborinate (DPBA) is a boronic ester that selectively forms a complex with flavonoid compounds that is fluorescent under excitation with UV light, the emission wavelength of which varies with the flavonoid used.[15] This compound can be used as a staining agent to image surfaces functionalized with flavonoids by fluorescence microscopy.[11]

We therefore considered that DPBA could also be used to determine the amount of flavonoid grafted to the surface, using a simple fluorescence spectrophotometer. Since DPBA is known to interact with a large amount of flavonoids, such as naringenin, kaempferol, phloretin, quercetin, and apigenin, among others,[15] the method presented here could be applied in the characterization of several plant-derived polyphenol coatings.

On the other hand, to promote tissue integration around an implant, a fast cell adhesion after the implantation is crucial.[16] Several fundamental cellular processes, such as cell migration, morphogenesis, proliferation, gene expression, and survival, are regulated by the adhesion of cells to a substrate, and the chemistry and topography of the implant surface affects cell adhesion.[17−20] Catechol functionalities have been related to the adherence properties of several materials, and surfaces with catechol moieties, such as polydopamine coatings, have shown enhanced hydrophilicity.[21] Surface wettability also affects cell−material interaction, and hydrophilic surfaces favor cell adhesion.[22] In our previous work, we observed that surfaces functionalized with flavonoids were more hydrophilic than control Ti substrates.[11] On the other hand, Choi et al.[23] confirmed the need for specific interactions between the catechol moieties and the cells when comparing surfaces with similar surface wettabilities, and proposed an adhesion mechanism dependent on the specific linkage between catechol and thiolated biological molecules such as proteins. We hypothesized here that quercitrin coatings could enhance a rapid cell adhesion due to the presence of cathecol groups on the surface.

The flavonoid quercitrin is a glycoside of quercetin and rhamnose, present in tartary buckwheat and in the bark of various species of oak trees. It is intensely yellow colored, and used in the dye quercitron. Quercitrin has been shown to protect the skin from UVB-induced oxidative damage,[24] and has also been administered therapeutically in inflammatory diseases such as colitis in vivo.[25] In our previous studies, this flavonoid showed the highest bioactive effects on different bone and gingival cells in vitro; therefore, we selected quercitrin for this work.[12−14]

The aims of the present work were (1) to develop a fluorescence-based surface quantification method for the determination of the amount of flavonoid grafted on the Ti surface using DPBA, a flavonoid-specific probe, (2) to optimize the quercitrin grafting procedure, and (3) to evaluate the biological effect in vitro of quercitrin nanocoatings on the adhesion, viability, and mineralization of hMSCs differentiated to the osteoblastic lineage. To optimize the quercitrin grafting procedure, we evaluated a reductive amination approach, using $NaCNBH_3$ as a reducing agent. This approach was validated by FTIR and XPS spectroscopy. Then we optimized the grafting conditions determining the amount of quercitrin grafted on the surfaces by the fluorescence spectroscopy method developed. Finally, we evaluated the biological effect of the quercitrin-nanocoated surfaces on the hMSC adhesion and mineralization. We found that quercitrin surfaces significantly promoted a faster initial cell adhesion than control Ti and aminosilanized surfaces (APTES, (3-aminopropyl)triethoxysilane, was used as a cross-linker molecule between Ti and quercitrin), increased cell viability, indicated by an increase in the metabolic activity of cells cultured on the quercitrin surfaces, and enhanced cell mineralization after 21 days of cell culture, as indicated by a higher calcium content and alkaline phosphatase (ALP) activity, as well as by a higher density of mineralized nodules.

EXPERIMENTAL SECTION

Materials. Machined Ti disks, c.p. grade IV, 6.2 mm diameter, and 2 mm height, were purchased from Implantmedia (Lloseta, Spain) and cleaned as follows: The coins were first immersed in water, followed by 70% ethanol, then in an ultrasonic bath at 40 °C for 5 min in water, and in 40% NaOH at 40 °C for 10 min, sonicated in water for 5 min, and washed with water until neutral pH of the water after use was reached Afterward, the disks were sonicated in water at 50 °C for 5 min, immersed in 50% HNO_3 at 50 °C for 10 min, and sonicated in warm water for another 5 min. Finally, the coins were washed with water until neutral pH, dried under a N_2 flow, and stored at room temperature until use.[26] For FTIR and XPS analysis the Ti disks were mirror polished prior to modification (Phoenix 4000, Buehler GmbH, Duesseldorf, Germany).[26] APTES, quercitrin hydrate, quercitrin standard, sodium cyanoborohydride in NaOH (5 M), DPBA, polyethylene glycol 4000 (PEG4000), and calcein blue were purchased from Sigma-Aldrich (St. Louis, MO). Deionized water was obtained from a Millipore system (Billerica, MA). Technical acetone and NaOH were purchased from Fisher Scientific (Madrid, Spain). Nitric acid (69.5%), absolute ethanol, and anhydrous toluene, reagent grade, were purchased from Scharlab (Barcelona, Spain). Hellmanex III solution was purchased from Hellma Hispania (Badalona, Spain).

Preparation of Quercitrin-Nanocoated Titanium Surfaces. Ti substrates were first passivated with 30% HNO_3 for 30 min, rinsed thoroughly with water, and left in water overnight. Then the coins were dried under a N_2 flow and immediately aminosilanized with 2% APTES in dry toluene for 24 h. To obtain QR samples (Figure 1), the aminosilanized surfaces were chemically functionalized with quercitrin by immersion in a quercitrin hydrate 1 mM aqueous solution (250 μL/coin) at pH 5.5 for 1 h, as previously described.[11] In this step, the reaction of the ketone moiety of the flavonoid with the terminal amine group of the silane at mildly acidic pH gave an imine (C═N) bond between the APTES cross-linker and the flavonoid. To optimize the quercitrin coating, the use of $NaCNBH_3$ to selectively reduce the imine bond between the flavonoid and the silane to a single C−N bond was evaluated. This way, QRred surfaces (Figure 1) were obtained in either one or two steps. In the two-step procedure, QR

DOI: 10.1021/acsami.5b05044
ACS Appl. Mater. Interfaces 2015, 7, 16857−16864

surfaces were prepared as described before, and further immersed in 50 μM $NaCNBH_{3aq}$ for 1 h at room temperature, rinsed twice with water, and dried under a N_2 flow. In the one-step procedure, passivated and aminosilanized Ti coins were immersed in aqueous solutions of quercitrin hydrate (1 mM, 250 μL/coin) at pH 7.5, containing $NaCNBH_3$ (50, 100, 200, or 400 μM) for different reaction times (30 min or 1 h) at room temperature. Then the samples were rinsed twice with water and dried under a N_2 flow. The samples were prepared in the most aseptic conditions possible. For the in vitro characterizations, QRred samples were obtained with the one-step procedure, using $NaCNBH_3$ (100 μM) and 1 h of grafting time.

FTIR Analysis. FTIR spectra were obtained on at least 10 random measurement points on each sample surface (resolution, 4 cm^{-1}; number of scans, 16, reference, Ti) with a Bruker Tensor 27 FTIR spectrophotometer (Bruker Española, Barcelona, Spain) coupled to a Hyperion 3000 UV−vis/IR microscope with an attenuated total reflection (ATR) objective. At least two sample replicates (n = 2) were analyzed for each group. Since reproducible and overlapping spectra were acquired in different points of the functionalized surfaces, the average spectrum of each group was calculated.

Quantification of Quercitrin Grafted to Titanium Surfaces by Fluorescence Spectroscopy. A stock solution of quercitrin standard (500 μM) was prepared in absolute ethanol. Aliquots of quercitrin standard stock solution were stored at −80 °C. Standard surfaces with a known amount of quercitrin were prepared by carefully drop casting a volume of stock solution containing a known amount of the biomolecule (0.1, 0.25, 0.5, 0.75, 1, or 1.5 nmol) on the surface of passivated Ti coins, which were further allowed to air-dry for 20 min. In a 96-well plate suitable for fluorescence measurements, the samples and standard surfaces were carefully stained with 5 μL of DPBA (22 mM) in methanol, followed by 5 μL of PEG4000 (5%, m/v) in ethanol. After 1.5 h, the fluorescence emission spectrum of the samples was acquired, from λ_{em} = 500 nm to λ_{em} = 700 nm, at excitation wavelength λ_{exc} = 480 nm, using a Varian Cary Eclipse fluorescence spectrophotometer with a microplate reader (Agilent Technologies, Santa Clara, CA). A calibration curve was obtained from the maximum fluorescence intensity at λ_{em} = 570 nm. Three sample and standard replicates (n = 3) were used in each analysis. Fluorescence images (λ_{ex} = 450−490 nm) were taken with a Leica DM R (Wetzla, Germany) fluorescence microscope and pseudocolored with Leica software.

XPS Measurements. XPS analyses on QRred surfaces were performed using a K-Alpha (Thermo Scientific) system, with a monochromatic Al Kα (1486.68 eV) X-ray source with a spot size of 300 μm and 50.4 W (12 kV × 4.2 mA) of power. For each sample, two survey spectra as well as a high-resolution spectrum were adquired for the C, O, N, and Ti elements. Two sample replicates (n = 2) were analyzed for each group.

Cell Culture. Human bone marrow stromal cells (hMSCs) (Stem Cell Technologies, Grenoble, France) were cultured at standard conditions of 37 °C and 5% CO_2, and maintained in low-glucose DMEM (Dulbecco's modified Eagle's medium) GlutaMAX cell culture medium (Life Technologies, Carlsbad, CA) supplemented with 10% stem-cell-tested fetal bovine serum (Biosera, Boussens, France), 100 $U{\cdot}mL^{-1}$ penicillin, and 100 $\mu g{\cdot}mL^{-1}$ streptomycin (Biowest, Nuaille, France). The supplier assured that the cells were obtained ethically and legally and that all donors provided written informed consent. Experiments were performed with hMSCs at passage 5 or 6 after isolation. At day 0, the coins were placed in 96-well plates and hMSCs were seeded at a density of 7.0 × 10^3 cells $well^{-1}$. The cells were cultured in culture medium until confluence at day 4, and then grown in culture medium supplemented with ascorbic acid (50 μg/mL) and dexamethasone (10 nM) (determination of metabolic activity) or hydrocortisone (100 nM) (determination of ALP activity, calcium content, and mineralized nodule formation by calcein blue staining) from day 4 until day 21.

Cytotoxicity Assays. After 24 h of culture, lactate dehydrogenase (LDH) activity in the culture medium was determined following the manufacturer's instructions (cytotoxicity detection kit, Roche Diagnostics, Mannheim, Germany). The results are presented relative to the LDH activity in the medium of cells cultured on tissue culture plastic in culture medium (low control, 0% cell death) and of cells treated with surfactant Triton X-100 (1%) (high control, 100% cell death), according to eq 1. Five sample replicates (n = 5) were analyzed for each group.

$$\text{cytotoxicity (\%)} = \frac{\text{exptl value} - \text{low control}}{\text{high control} - \text{low control}} \times 100 \quad (1)$$

Cell Adhesion and Metabolic Activity. Cell adhesion and metabolic activity were quantified using PrestoBlue, a live-cell resazurin-based viability reagent (Life Technologies, Carlsbad, CA). When added to the medium, the reducing environment within viable cells converts the PrestoBlue reagent to an intensely red fluorescent dye, and this change can be spectrophotometrically determined. To determine cell adhesion, Ti sample coins were placed in 96-well plates and the cells were seeded at a density of 7.0 × 10^3 cells $well^{-1}$. Four sample replicates of two different batches (n = 4) were used. Time 0 was set when the first well was seeded with cells. At adhesion times of 15, 30, 60, and 120 min, the medium was aspirated, the cells were washed twice with PBS, and 100 μL of fresh culture medium was added to each well. Right after the last time point (120 min), 10 μL of PrestoBlue was added to all samples, as well as to wells containing a known amount of cells (standards), and the samples and standards were incubated at 37 °C overnight. Cell standards were prepared in triplicate. The day after, the absorbance of the medium was read at 570 and 600 nm, and the cell number was calculated, following the manufacturer's protocols. The total metabolic activity was determined at 1, 6, 14, and 21 days of hMSC culture on the surfaces, on six sample replicates of each group (n = 6), adding 10 μL of PrestoBlue to cells with 100 μL of culture medium and reading the absorbance of the medium at 570 and 600 nm after 1 h of reagent incubation time at 37 °C, following the manufacturer's protocols.

ALP Activity, Calcium Content, and Calcein Blue Staining. The ALP activity and total calcium content of hMSCs after 21 days of culture were determined from cell lysates as described previously,[27] using three replicates of two different sample batches (n = 3). Bonelike nodule formation was evaluated by calcein blue staining of two sample replicates (n = 2), following the procedure reported by Goto et al.:[28] A 10 mg portion of calcein blue was dissolved in 0.25 mL of KOH (1 M), and 9.75 mL of distilled water was added to obtain a 3.1 × 10^{-3} M calcein blue solution. The solution was filtered through a 0.22 μm membrane and added to the culture medium (15 μL per well, to achieve a final concentration in each well of 3.1 × 10^{-5} M), and the culture was incubated for 1 h at 37 °C. Then the surfaces were thoroughly washed with PBS, fixed with p-formaldehyde (4%) in PBS for 10 min, washed again with PBS, and air-dried. Stained coins were then glued to microscope slides, and representative fluorescence images of each surface were acquired with a confocal microscope (Leica DMI 4000B equipped with a Leica TCS SPE laser system) under UV light excitation.

Statistics. Differences between groups were assessed by the Mann−Whitney test or by the Student t test depending on their normal distribution. The Kolmogorov−Smirnov test was used to assume parametric or nonparametric distributions for the normality tests. The software SPSS v.17.0 (SPSS, Chicago, IL) was used to perform the tests. The results were considered statistically significant at $p \leq 0.05$.

RESULTS AND DISCUSSION

Functionalization of Titanium Surfaces with Quercitrin. The surface of Ti coins was functionalized with quercitrin, using an aminosilane as a cross-linker, followed by two different reaction conditions for the grafting of the flavonoid (Figure 1). QR surfaces were obtained as reported previously,[11] by reaction of the ketone moiety of the flavonoid with the terminal amine group of the silane at mildly acidic pH, giving an imine (C═N) bond by the formation of a Schiff base. Since imine bonds are reversible and can be hydrolyzed, we explored here a reductive amination approach to graft the flavonoid to the surface. This

DOI: 10.1021/acsami.5b05044
ACS Appl. Mater. Interfaces 2015, 7, 16857−16864

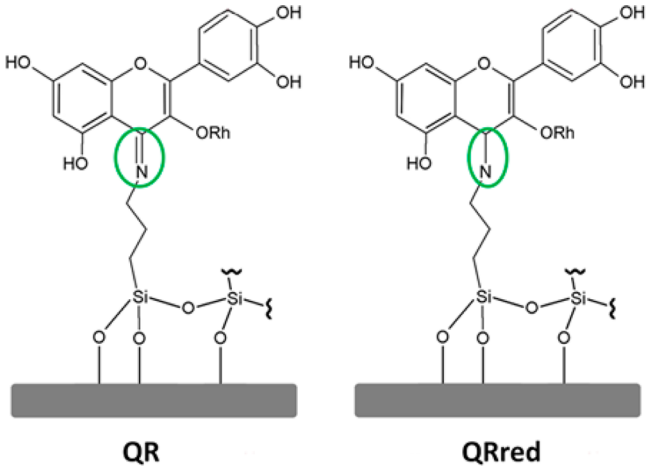

Figure 1. Functionalization of Ti substrates with quercitrin. The reaction of the ketone moiety of quercitrin with the terminal amine of the APTES silane gave an imine (C═N) bond between the biomolecule and the cross-linker (QR surfaces). When $NaCNBH_3$ was added to the reaction medium, the imine bond was selectively reduced to a single C−N bond (QRred surfaces). Rh = rhamnose.

way, we expected that the use of the reducing agent $NaCNBH_3$ in the flavonoid grafting reaction would reduce the imine bond between quercitrin and the silane to a simple, less reactive, and irreversible C−N bond (QRred surfaces). Initially, we defined the concentration of reducing agent $NaCNBH_3$ as 50 μM, according to the work of Razumovitch et al.,[29] and performed the quercitrin grafting reaction, followed by the addition of the reducing agent, in a two-step procedure. To evaluate the viability of this approach, we characterized the surfaces obtained by FTIR and XPS spectroscopy (Figure 2 and Figure 3).

Figure 2 shows the average FTIR spectra obtained on the different surfaces, before the reduction step (QR) and after the

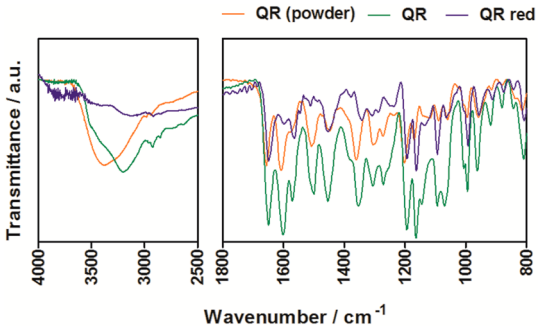

Figure 2. Average FTIR spectra of quercitrin-modified Ti surfaces, obtained with (QR red) or without (QR) reducing agent, compared to the spectrum of the pure compound (QR powder). Two sample replicates were analyzed for each group (n = 2), and spectra were acquired on at least 10 surface measurement points of each sample replicate.

reduction step with $NaCNBH_3$ (QRred), compared to the spectrum of pure quercitrin. The bands present in the FTIR spectra of both quercitrin-modifed surfaces overlapped with those of the pure compound, indicating the presence of quercitrin on both QR and QRred surfaces, in addition to bands representative of the APTES molecule, used as a cross-linker. The bands at 2936 and 2870 cm^{-1} were assigned to the vibrations of the alkyl chain of the aminosilane. The detailed analysis of the FTIR spectra of the intermediate APTES surfaces, and the nonreduced quercitrin-modifed surfaces, was reported in our previous work.[11] The wide band present at 3100 cm^{-1} indicated the presence of N−H bonds in both quercitrin-modified surfaces. In QRred surfaces, the spectra also showed a medium-intensity band at 1570 cm^{-1} that may correspond to the vibration of a N−H bond of a secondary amine, and could be due to the successful reduction of the imine. It can also be noticed that the intensity of the band at 1600 cm^{-1} decreased for QRred surfaces. This may be due to a loss of conjugation of the condensed aromatic nuclei of the flavonoid, and would also be in accordance with the presence of a single C−N bond between the biomolecule and the silane.

The atomic composition of the surface of QRred samples was determined by XPS and gave a C1s atomic content of 52.6%, an O1s content of 33.1%, a Ti2p content of 6.63%, a N1s content of 3.47%, and a Si2p content of 4.17%. These results were similar to those obtained on QR surfaces (a C1s content of 60.7%, an O1s content of 29.5%, a Ti2p content of 2.3%, a N1s content of 3.18%, and a Si2p content of 4.14%), reported previously,[11] and indicate the presence of both quercitrin and the silane on the Ti surface. The increase in the titanium content of the reduced samples, together with the decrease in its carbon content, in comparison to that of the nonreduced QR surfaces, could indicate a lower amount of biomolecule grafted on the QRred surfaces. Figure 3 shows the

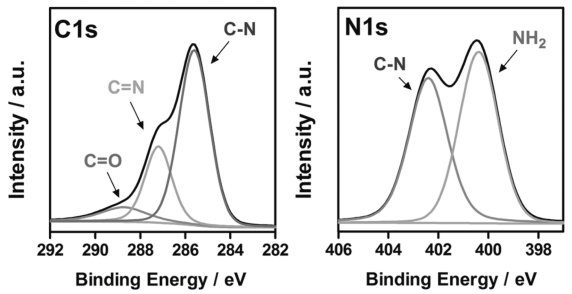

Figure 3. Deconvolution of C1s and N1s XPS high-resolution peaks of QRred surfaces indicated the presence of a single C−N bond between the biomolecule and the silane. Two sample replicates were analyzed (n = 2).

deconvolution of C1s and N1s XPS high-resolution peaks of QRred surfaces. The C1s peak showed three contributions, one related to the presence of C═O carbonyl groups from ambient contaminations or nonreacted quercitrin, and the other two related to C═N and C−N bonds on the surface. Although both bonds appeared, there was a 64% content of the C−N bond versus a 26% content of the C═N bond. On the other side, the deconvolution of the N1s peak showed two contributions, related to the presence of C−N bonds and free amine groups of the silane layer. These results point to the successful reduction of the imine bond of QR surfaces to a single C−N bond between the biomolecule and the silane in QRred samples and the viability of the reductive amination approach to fabricate quercitrin-modified surfaces.

Quantification of the Amount of Quercitrin on the Surfaces by Fluorescence Spectroscopy. With the aim of quantifying the quercitrin density on the modified Ti surfaces, we developed a surface quantification method based on fluorescence spectroscopy. The method uses DPBA, a flavonoid-specific probe that spontaneously forms a fluorescent

DOI: 10.1021/acsami.5b05044
ACS Appl. Mater. Interfaces 2015, 7, 16857−16864

complex with flavonoid compounds and that is commonly used for the detection and identification of flavonoids by thin-layer chromatography, for the imaging of their localization in plants[15,30] and, more recently, to visualize and to quantify flavonoid intake by cells in vitro.[31−33] To obtain a suitable calibration curve, we prepared several standard surfaces containing known amounts of quercitrin, from 0.1 to 1.5 nmol per surface, on 6.2 mm diameter Ti coins, by drop casting a known volume of a standard quercitrin solution on a known area of Ti substrate and allowing it to air-dry, in an approach similar to that proposed by Borguet et al. to quantify functional groups on surfaces by fluorescence spectroscopy.[34−36] The quercitrin standard surfaces were carefully stained with a methanolic solution of DPBA (22 mM), followed by the addition of a PEG4000 (5%, m/v) solution in ethanol to the stained surfaces, to stabilize the fluorescence intensity. After 1.5 h of the staining, fluorescence emission spectra were acquired at an excitation wavelength of 480 nm (Figure 4), and a linear

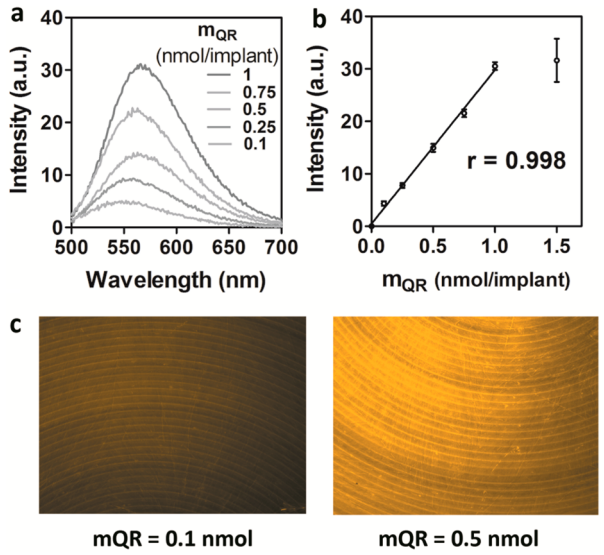

Figure 4. (a) Fluorescence emission spectra of standard surfaces with known amounts of quercitrin on Ti substrates of 6.2 mm diameter, at λ_{exc} = 480 nm, after 1.5 h of being stained with DPBA (22 mM) in methanol and PEG4000 (5%, m/v) in ethanol. A light shift of the maximum wavelength due to concentration effects was observed. (b) There was a linear relationship between the fluorescence intensity at λ_{em} = 570 nm and the amount of quercitrin dropped on the Ti surface, until 1 nmol per coin. After that, fluorescence quenching occurred. Three sample replicates of each standard point were used (n = 3). (c) Pseudocolored fluorescence images of standard surfaces with 0.1 and 0.5 nmol of quercitrin per coin. Fluorescence was homogeneous and covered all the coin area for all standards.

correlation between the fluorescence intensity and the amount of quercitrin drop casted on the surface was observed, at an emission wavelength of 570 nm, with correlation coefficients higher than 0.99 until 1 nmol of quercitrin per coin. At higher amounts of quercitrin, a quenching of the fluorescence occurred and the fluorescence intensity decreased. Quercitrin coatings without DPBA did not emit fluorescence, and neither did APTES and Ti surfaces with and without DPBA.

Using this fluorescence-based method, we successfully quantified the quercitrin grafted on QR and QRred surfaces, and varied the reaction conditions to optimize the surface functionalization procedure. The results are shown in Table 1.

Table 1. Amount of Quercitrin Grafted on Ti Surfaces, As Determined by Fluorescence Spectroscopy after Staining with DPBA and PEG4000, for Different Reaction Conditions[a]

	quercitrin reaction conditions			
grafting strategy	no. of steps	[$NaCNBH_3$] (μM)	time (h)	m_{QR} (pmol/coin)
QR		nonvaried		167 ± 136
				613 ± 569
				842 ± 361
QRred	2	50	1	nd[b]
	1	50	1	110 ± 18
	1	100	1	172 ± 45
	1	200	1	19 ± 24
	1	400	1	<10
	1	100	0.5	71 ± 39
	1	100	1	74 ± 4
	1	100	1	64 ± 10

[a]The results of independent experiments are presented, and three replicates were measured for each independent experiment (n = 3). [b]Inconsistent results.

The amount of quercitrin on QR surfaces was variable between experiments and sample replicates, between 167 ± 136 and 842 ± 361 pmol per coin. Regarding QRred surfaces, we evaluated two-step and one-step grafting procedures. In the two-step procedure, quercitrin coatings were obtained following the QR procedure, and then the samples were immersed in a reducing $NaCNBH_3$ solution. In the one-step procedure, quercitrin and $NaCNBH_3$ were simultaneously added to the reaction medium, where the aminosilanized samples were immersed. Using the two-step procedure, we could not quantify the amount of flavonoid on the surface; some samples were under the detection limit, while others showed inconsistent replicate results. On the contrary, using the one-step reaction, consistent results were obtained. At $NaCNBH_3$ concentrations of 50 and 100 μM, the grafting reaction succeeded and the amount of quercitrin was between 64 ± 10 and 172 ± 45 pmol per coin. Increasing $NaCNBH_3$ concentrations impaired the immobilization of the flavonoid. The amounts of flavonoid on QRred surfaces were lower than on QR, but more reproducible. The lower amount of quercitrin grafted on QRred surfaces could be due to the poor hydrolytic stability of siloxanes at pH 7.5.[37] Since QRred surfaces were fabricated at neutral pH, and this may favor the hydrolysis of the APTES coupling layer, less amine groups would be available on the surface for the grafting of the flavonoid.

Biological Behavior of Quercitrin-Nanocoated Surfaces in Vitro. To compare the bioactivity of QR and QRred quercitrin nanocoatings, we evaluated the behavior of hMSCs cultured in vitro on quercitrin-modified Ti surfaces, studying the effect of the surfaces functionalized with quercitrin on cell adhesion, viability, and mineralization of bone-marrow-derived hMSCs after 21 days of cell culture. QRred samples were obtained here following the one-step procedure, using $NaCNBH_3$ (100 μM) and 1 h of grafting time.

First, the cytotoxicity of QRred surfaces was evaluated after 1 day of cell culture on the surfaces by measuring the activity of LDH, and compared to that of the other surfaces studied. QRred surfaces were not toxic for the cells, as indicated by a percentage cytotoxicity of 13.9 ± 2.5%, similarly to the other surface groups (Figure S1, Supporting Information).

DOI: 10.1021/acsami.5b05044
ACS Appl. Mater. Interfaces 2015, 7, 16857−16864

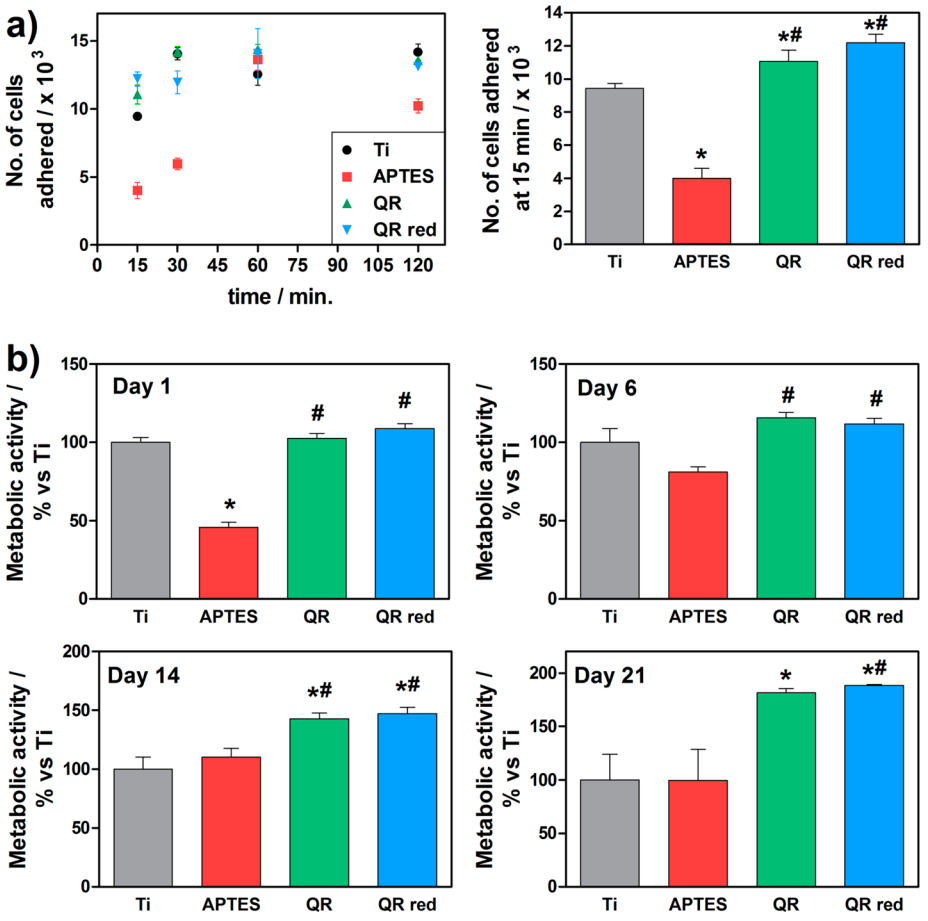

Figure 5. (a) Quercitrin-modified surfaces promoted a faster stem cell adhesion compared to Ti and APTES control surfaces. The graph on the left shows the number of cells adhered on the surfaces at 15, 30, 60, and 120 min of cell seeding. The graph on the right shows a detail of the number of cells adhered after 15 min of cell seeding. (b) Metabolic activity of cells cultured on QR and QRred surfaces increased along the cell culture period. Values represent the mean ± SEM, with $n = 4$ for cell adhesion and $n = 6$ for metabolic activity. t test: *, $p < 0.05$ vs Ti; #, $p < 0.05$ vs APTES.

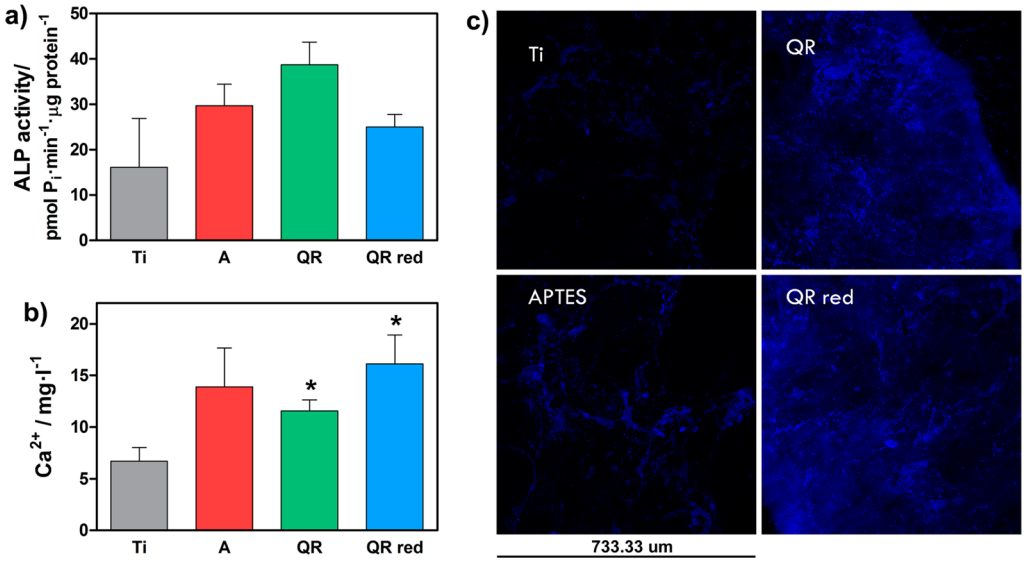

Figure 6. Mineralization was promoted in hMSCs cultured on both QR and QRred surfaces after 21 days of cell culture, as indicated by the (a) ALP activity, (b) calcium content of cell lysates, and (c) fluorescence images after calcein blue staining of the mineralization nodules formed on the surfaces. Values represent the mean ± SEM, with $n = 3$ for ALP activity and Ca^{2+} content and $n = 2$ for calcein blue staining. t test: *, $p < 0.05$ vs Ti.

Cell adhesion is a very important issue in implant surfaces. A rapid cell adhesion after the implantation can improve the integration of the surrounding tissues and decrease the chances of bacteria colonizing on the surface.[16] Figure 5 shows that hMSCs adhered faster to the surfaces functionalized with quercitrin compared to Ti and APTES control surfaces. After

DOI: 10.1021/acsami.5b05044
ACS Appl. Mater. Interfaces 2015, 7, 16857−16864

15 min of cell seeding, almost all the cells seeded were adhered to QR and QRred surfaces, while less were adhered to Ti, and few to the aminosilanized APTES surface. After 60 min of cell seeding, all the groups reached the maximum cell adhesion. We attributed the greater initial stem cell adhesion observed on quercitrin-nanocoated surfaces to the presence of the catechol groups of the flavonoid on the surface, since this chemical moiety is related to the adhesion properties of several kinds of materials.[21] The presence of catechol groups on biomaterial surfaces has also shown improved cell adhesion of fibroblast cells.[38,39] Since a fast cell adhesion to the biomaterial surface is key to win the "race for the surface" against bacteria, these results indicate the potential of quercitrin-nanocoated implant surfaces to induce a rapid and successful osseointegration.

Cell viability on the different surfaces was evaluated at days 1, 6, 14, and 21 of cell culture by measuring the metabolic activity of cells using a live cell colorimetric assay (Figure 5b). We found an increased metabolic activity of cells cultured on both QR and QRred surfaces along the cell culture period compared to Ti and APTES control surfaces. Therefore, quercitrin nanocoatings induced a higher cell viability that could be related to the faster cell adhesion observed on these surfaces.

Finally, we assessed the effect of the surfaces on the mineralization degree of hMSCs after 21 days of cell culture (Figure 6), determining the activity of alkaline phosphatase and the calcium content from cell lysates, together with the staining of mineralized nodules formed on the different group surfaces by calcein blue.

Both QR and QRred surfaces showed increased ALP activity compared to Ti control surfaces, although no statistically significant difference was achieved. The calcium content of cells cultured on both QR and QRred surfaces was significantly higher compared to that of the control Ti, and agreed with the fluorescence staining of the mineralized nodules, which indicated a higher cell mineralization on the quercitrin-modified surfaces. ALP is an early marker of osteoblast differentiation that is involved in hydroxyapatite crystal deposition; its expression increases during extracellular matrix maturation and decreases when mineralization is well progressed, which is consistent with the results obtained herein.[40] Aminosilanized surfaces also showed an increased ALP activity and calcium content compared to Ti, although they did not reach significant difference, and calcein blue fluorescence staining did not show as much cell mineralization on APTES surfaces as on quercitrin-nanocoated surfaces. Besides, the mineralization results obtained here with bone-marrow-derived hMSCs cultured on QR and APTES surfaces agreed with our previous results with umbilical-cordon-derived hMSCs. Furthermore, although the flavonoid density on QRred surfaces was lower than in QR samples, the results obtained indicate that QRred surfaces promoted the mineralization of hMSCs similarly to QR surfaces.

CONCLUSIONS

We have developed a fluorescence-based method to quantify the amount of quercitrin grafted to titanium surfaces using a flavonoid-specific dye, DPBA. The method is simple and rapid and can detect subnanomolar amounts of quercitrin, using routine characterization equipment present in any research laboratory. We believe this method could be extended to the quantification of other polyphenol-based thin coatings on several surfaces.

We used an alternative approach for the covalent functionalization of Ti subtrates with quercitrin based on reductive amination, using $NaCNBH_3$ as a selective reducing agent. The amount of quercitrin grafted to the surface was lower than that using our previous grafting procedure, even though the biological effect on hSMCs was similar for the two quercitrin-modified groups.

Quercitrin-modified Ti surfaces significantly promoted stem cell adhesion and osteoblast mineralization in vitro, compared to Ti and aminosilanized control surfaces. Cell adhesion to a biomaterial is dramatically important, since it influences several processes such as cell migration, proliferation, gene expression, and cell function. Furthermore, a rapid cell adhesion can decrease the chances of bacteria colonizing on an implant surface. Thus, although further in vivo experiments should be performed to confirm these results, these bioactive surfaces could be used to promote a rapid osseointegration of bone implants, decreasing implant failure risk.

ASSOCIATED CONTENT

Supporting Information

Cytotoxicity of the surfaces measured by LDH activity after 1 day of culturing hMSCs on the surfaces. The Supporting Information is available free of charge on the ACS Publications website at DOI: 10.1021/acsami.5b05044.

AUTHOR INFORMATION

Corresponding Authors

*E-mail: marta.monjo@uib.es.
*E-mail: joana.ramis@uib.es.

Notes

The authors declare the following competing financial interest(s): A.C., M.M., and J.M.R. are inventors of a pending patent application based on some aspects of this work (PCT/EP2013/058116).

ACKNOWLEDGMENTS

This work was supported by the Conselleria d'Educació, Cultura i Universitats del Govern de les Illes Balears, and the European Social Fund (contract to J.M.R.). We acknowledge NANBIOSIS ICTS (CIBER-BBN) and SACSS-SAIUEx (UEx) for the use of the XPS facility.

REFERENCES

(1) Yang, Z.; Xiong, K.; Qi, P.; Yang, Y.; Tu, Q.; Wang, J.; Huang, N. Gallic Acid Tailoring Surface Functionalities of Plasma-Polymerized Allylamine-Coated 316L SS to Selectively Direct Vascular Endothelial and Smooth Muscle Cell Fate for Enhanced Endothelialization. *ACS Appl. Mater. Interfaces* **2014**, *6*, 2647−2656.

(2) Xiao, L.; Mertens, M.; Wortmann, L.; Kremer, S.; Valldor, M.; Lammers, T.; Kiessling, F.; Mathur, S. Enhanced in Vitro and in Vivo Cellular Imaging with Green Tea Coated Water-Soluble Iron Oxide Nanocrystals. *ACS Appl. Mater. Interfaces* **2015**, *7*, 6530−6540.

(3) Kim, S.; Kwak, S.; Lee, S.; Cho, W. K.; Lee, J. K.; Kang, S. M. One-Step Functionalization of Zwitterionic poly[(3-(methacryloylamino)propyl)dimethyl(3-Sulfopropyl)ammonium Hydroxide] Surfaces by Metal-polyphenol Coating. *Chem. Commun. (Cambridge, U. K.)* **2015**, *51*, 5340−5342.

(4) Lu, Y.-C.; Luo, P.-C.; Huang, C.-W.; Leu, Y.-L.; Wang, T.-H.; Wei, K.-C.; Wang, H.-E.; Ma, Y.-H. Augmented Cellular Uptake of Nanoparticles Using Tea Catechins: Effect of Surface Modification on Nanoparticle-Cell Interaction. *Nanoscale* **2014**, *6*, 10297−10306.

(5) Daglia, M. Polyphenols as Antimicrobial Agents. *Curr. Opin. Biotechnol.* **2012**, *23*, 174−181.

DOI: 10.1021/acsami.5b05044
ACS Appl. Mater. Interfaces 2015, 7, 16857−16864

(6) Amić, D.; Davidović-Amić, D.; Beslo, D.; Rastija, V.; Lucić, B.; Trinajstić, N. SAR and QSAR of the Antioxidant Activity of Flavonoids. *Curr. Med. Chem.* **2007**, *14*, 827−845.
(7) Sileika, T. S.; Barrett, D. G.; Zhang, R.; Lau, K. H. A.; Messersmith, P. B. Colorless Multifunctional Coatings Inspired by Polyphenols Found in Tea, Chocolate, and Wine. *Angew. Chem., Int. Ed.* **2013**, *52*, 10766−10770.
(8) Hong, S.; Yeom, J.; Song, I. T.; Kang, S. M.; Lee, H.; Lee, H. Pyrogallol 2-Aminoethane: A Plant Flavonoid-Inspired Molecule for Material-Independent Surface Chemistry. *Adv. Mater. Interfaces* **2014**, *1*, 1400113.
(9) Barrett, D. G.; Sileika, T. S.; Messersmith, P. B. Molecular Diversity in Phenolic and Polyphenolic Precursors of Tannin-Inspired Nanocoatings. *Chem. Commun. (Cambridge, U. K.)* **2014**, *50*, 7265−7268.
(10) Ejima, H.; Richardson, J. J.; Liang, K.; Best, J. P.; van Koeverden, M. P.; Such, G. K.; Cui, J.; Caruso, F. One-Step Assembly of Coordination Complexes for Versatile Film and Particle Engineering. *Science* **2013**, *341*, 154−157.
(11) Córdoba, A.; Satué, M.; Gómez-Florit, M.; Hierro-Oliva, M.; Petzold, C.; Lyngstadaas, S. P.; González-Martín, M. L.; Monjo, M.; Ramis, J. M. Flavonoid-Modified Surfaces: Multifunctional Bioactive Biomaterials with Osteopromotive, Anti-Inflammatory, and Anti-Fibrotic Potential. *Adv. Healthcare Mater.* **2015**, *4*, 540−549.
(12) Satué, M.; Arriero, M. D. M.; Monjo, M.; Ramis, J. M. Quercitrin and Taxifolin Stimulate Osteoblast Differentiation in MC3T3-E1 Cells and Inhibit Osteoclastogenesis in RAW 264.7 Cells. *Biochem. Pharmacol.* **2013**, *86*, 1476−1486.
(13) Gómez-Florit, M.; Monjo, M.; Ramis, J. M. Quercitrin for Periodontal Regeneration: Effects on Human Gingival Fibroblasts and Mesenchymal Stem Cells. **2015**, manuscript in preparation.
(14) Gómez-Florit, M.; Monjo, M.; Ramis, J. M. Identification of Quercitrin as Potential Therapeutic Agent for Periodontal Applications. *J. Periodontol.* **2014**, *85*, 966−974.
(15) Murphy, a; Peer, W. a; Taiz, L. Regulation of Auxin Transport by Aminopeptidases and Endogenous Flavonoids. *Planta* **2000**, *211*, 315−324.
(16) Gristina, A. G. Biomaterial-Centered Infection: Microbial Adhesion versus Tissue Integration. *Science* **1987**, *237*, 1588−1595.
(17) Keselowsky, B. G.; Collard, D. M.; García, A. J. Surface Chemistry Modulates Fibronectin Conformation and Directs Integrin Binding and Specificity to Control Cell Adhesion. *J. Biomed. Mater. Res., Part A* **2003**, *66*, 247−259.
(18) Dalby, M. J.; Gadegaard, N.; Oreffo, R. O. C. Harnessing Nanotopography and Integrin-Matrix Interactions to Influence Stem Cell Fate. *Nat. Mater.* **2014**, *13*, 558−569.
(19) Discher, D. E.; Janmey, P.; Wang, Y.-L. Tissue Cells Feel and Respond to the Stiffness of Their Substrate. *Science* **2005**, *310*, 1139−1143.
(20) Provenzano, P. P.; Keely, P. J. Mechanical Signaling through the Cytoskeleton Regulates Cell Proliferation by Coordinated Focal Adhesion and Rho GTPase Signaling. *J. Cell Sci.* **2011**, *124*, 1195−1205.
(21) Sedõ, J.; Saiz-Poseu, J.; Busqué, F.; Ruiz-Molina, D. Catechol-Based Biomimetic Functional Materials. *Adv. Mater.* **2013**, *25*, 653−701.
(22) Anselme, K. Osteoblast Adhesion on Biomaterials. *Biomaterials* **2000**, *21*, 667−681.
(23) Choi, J. S.; Messersmith, P. B.; Yoo, H. S. Decoration of Electrospun Nanofibers with Monomeric Catechols to Facilitate Cell Adhesion. *Macromol. Biosci.* **2014**, *14*, 270−279.
(24) Yin, Y.; Li, W.; Son, Y.-O.; Sun, L.; Lu, J.; Kim, D.; Wang, X.; Yao, H.; Wang, L.; Pratheeshkumar, P.; Hitron, A. J.; Luo, J.; Gao, N.; Shi, X.; Zhang, Z. Quercitrin Protects Skin from UVB-Induced Oxidative Damage. *Toxicol. Appl. Pharmacol.* **2013**, *269*, 89−99.
(25) Comalada, M.; Camuesco, D.; Sierra, S.; Ballester, I.; Xaus, J.; Gálvez, J.; Zarzuelo, A. In Vivo Quercitrin Anti-Inflammatory Effect Involves Release of Quercetin, Which Inhibits Inflammation through down-Regulation of the NF-κB Pathway. *Eur. J. Immunol.* **2005**, *35*, 584−592.
(26) Lamolle, S. F.; Monjo, M.; Lyngstadaas, S. P.; Ellingsen, J. E.; Haugen, H. J. Titanium Implant Surface Modification by Cathodic Reduction in Hydrofluoric Acid: Surface Characterization and in Vivo Performance. *J. Biomed. Mater. Res., Part A* **2009**, *88*, 581−588.
(27) Satué, M.; Petzold, C.; Córdoba, A.; Ramis, J. M.; Monjo, M. UV Photoactivation of 7-Dehydrocholesterol on Titanium Implants Enhances Osteoblast Differentiation and Decreases Rankl Gene Expression. *Acta Biomater.* **2013**, *9*, 5759−5770.
(28) Goto, T. In Vitro Assay of Mineralized-Tissue Formation on Titanium Using Fluorescent Staining with Calcein Blue. *Biomaterials* **2003**, *24*, 3885−3892.
(29) Razumovitch, J.; De França, K.; Kehl, F.; Wiki, M.; Meier, W.; Vebert, C. Optimal Hybridization Efficiency upon Immobilization of Oligonucleotide Double Helices. *J. Phys. Chem. B* **2009**, *113*, 8383−8390.
(30) Buer, C. S.; Muday, G. K.; Djordjevic, M. a. Flavonoids Are Differentially Taken up and Transported Long Distances in Arabidopsis. *Plant Physiol.* **2007**, *145*, 478−490.
(31) Nifli, A. P.; Theodoropoulos, P. a.; Munier, S.; Castagnino, C.; Roussakis, E.; Katerinopoulos, H. E.; Vercauteren, J.; Castanas, E. Quercetin Exhibits a Specific Fluorescence in Cellular Milieu: A Valuable Tool for the Study of Its Intracellular Distribution. *J. Agric. Food Chem.* **2007**, *55*, 2873−2878.
(32) Ernst, I. M. a; Wagner, a. E.; Lipinski, S.; Skrbek, S.; Ruefer, C. E.; Desel, C.; Rimbach, G. Cellular Uptake, Stability, Visualization by "Naturstoff Reagent A", and Multidrug Resistance Protein 1 Gene-Regulatory Activity of Cyanidin in Human Keratinocytes. *Pharmacol. Res.* **2010**, *61*, 253−258.
(33) Lee, J. H.; Kim, Y.; Hoang, M. H.; Jun, H.; Lee, S.-J. Rapid Quantification of Cellular Flavonoid Levels Using Quercetin and a Fluorescent Diphenylboric Acid 2-Amino Ethyl Ester Probe. *Food Sci. Biotechnol.* **2014**, *23*, 75−79.
(34) McArthur, E. a.; Ye, T.; Cross, J. P.; Petoud, S.; Borguet, E. Fluorescence Detection of Surface-Bound Intermediates Produced from UV Photoreactivity of Alkylsiloxane SAMs. *J. Am. Chem. Soc.* **2004**, *126*, 2260−2261.
(35) Dementev, N.; Feng, X.; Borguet, E. Fluorescence Labeling and Quantification of Oxygen-Containing Functionalities on the Surface of Single-Walled Carbon Nanotubes. *Langmuir* **2009**, *25*, 7573−7577.
(36) Xing, Y.; Borguet, E. Specificity and Sensitivity of Fluorescence Labeling of Surface Species. *Langmuir* **2007**, *23*, 684−688.
(37) Silverman, B. M.; Wieghaus, K. a.; Schwartz, J. Comparative Properties of Siloxane vs Phosphonate Monolayers on a Key Titanium Alloy. *Langmuir* **2005**, *21*, 225−228.
(38) Choi, J. S.; Messersmith, P. B.; Yoo, H. S. Decoration of Electrospun Nanofibers with Monomeric Catechols to Facilitate Cell Adhesion. *Macromol. Biosci.* **2014**, *14*, 270−279.
(39) Xu, J. X.; Zhou, Z.; Wu, B.; He, B. F. Enzymatic Formation of a Novel Cell-Adhesive Hydrogel Based on Small Peptides with a Laterally Grafted L-3,4-Dihydroxyphenylalanine Group. *Nanoscale* **2014**, *6*, 1277−1280.
(40) Lian, J. B.; Stein, G. S. Development of the Osteoblast Phenotype: Molecular Mechanisms Mediating Osteoblast Growth and Differentiation. *Iowa Orthop. J.* **1995**, *15*, 118−140.

DOI: 10.1021/acsami.5b05044
ACS Appl. Mater. Interfaces 2015, 7, 16857−16864